ELSEVIER

Journal of Electrostatics 34 (1995) 205–224

Journal of
ELECTROSTATICS

The electrostatics of parachutes

Mark N. Horenstein[a,*], Norman Roberts[b]

[a] *Boston University, 44 Cummington St., Boston, MA 02215, USA*
[b] *US Army Natick Research, Development, and Engineering Center, STRNC-UE, Natick, MA 01760-5017, USA*

Received 12 April 1993; accepted after revision 13 September 1993

Abstract

Parachutes play an important role in many military operations involving personnel and equipment. Parachute designers have long suspected that nylon fabric may acquire enough electrostatic charge to impede or even prevent parachute opening. The work reported here seeks to determine the conditions, if any, under which electrostatic effects become important during parachute opening.

A simple Bernoulli model is used to estimate the principal aerodynamic forces during the early stages of inflation. Electrostatic forces are estimated using a variety of models, including a double layer model for two folds of charged parachute fabric, a vertical charge slab model for a separated parachute gore, and a discretized model for the peeling folds of a parachute gore. The various models are used to predict the minimum airspeed required to open a charged parachute. Theoretical results are compared with actual measurements of a small-scale charged parachute deployed in a wind tunnel.

Forward

This paper describes theory and experiments designed to investigate the possible effects of electrostatic charge on the initial stages of parachute inflation. The problem is a messy one plagued by uncertainty, agitated by air turbulence, and fraught with unknown charge everywhere. It is the type of problem that Jim Melcher would have loved. His ability to seek out the essence of a complicated problem, reducing it to a set of simple models verifiable by experiment, was one of the principal lessons that he taught his students. Much of the progress reported in the present body of work follows a problem approach advocated by Prof. Melcher. We are pleased that this paper could be included in this special issue of the *Journal of Electrostatics* – a fitting tribute to a great experimentalist, theorist, mentor, and remarkable individual.

* Corresponding author.

SSDI 0304-3886(94)00034-4

1. Introduction

The standard circular canopy parachute, essentially unchanged since the 1940s, still forms the cornerstone of most military airdrops involving personnel and equipment. Parachutes are made of nylon, a material known for its ability to acquire and retain electrostatic charge. Parachute designers have long suspected that electrostatic attraction – "static cling" – may act to impede the opening of parachutes or lead to catastrophic failure under certain circumstances. Despite this widely held suspicion, few references to electrostatic effects can be found in the literature and none appear in the various publications relating to electrostatics. In his classic reference book on parachutes, Brown [1] briefly cites the nuisance effect of electrostatics on parachute packing. Another well documented 1955 study [2], performed at the Lowell Technological Institute, investigated commercial antistatic agents for use on parachute fabrics. Although this study indicated previous interest in the problem, the work was limited to measurements of surface resistivity on cloth samples subjected to various treatment agents and did not fundamentally address the effect of electrostatic charge on the parachute opening process. A handful of reports from Airdrop Review and Malfunction Safety Analysis [3], a compendium of military airdrop equipment failures, allude to the possible role of electrostatics in parachute failure. One of these reports cited possible "air starvation due to static electricity" as a cause of failure and recommended "historical research of cold climate drops to identify if there is a real problem". Another report speculates, "Due to high temperature and intermitting showers we suspect static electricity prevented the parachute from fully opening". These reports are purely speculative, however, and none reaches a definitive conclusion concerning the effects of electrostatic charge on parachutes.

A 1983 study [4] performed for the US Army Natick Research, Development, and Engineering Center concluded that charge on rectangular samples of parachute cloth can be generated by triboelectrification under forces normally encountered during the opening process and that such charge can exert reasonable force. Aerodynamic and electrostatic forces were not compared in this study, however, hence no conclusion could be reached concerning the significance of electrostatic forces in retarding or preventing full parachute opening.

At present, no known parachute failure can be unequivocally attributed to electrostatic effects. Nevertheless, the suspicion has persisted that electrostatic attraction of oppositely-charged cloth surfaces may act to impede parachute opening under extremes of low humidity, low temperature, or atmospheric electrical disturbances. The goal of the ongoing research reported here is to determine the conditions, if any, under which electrostatic forces become comparable to or exceed aerodynamic forces and hence may retard or prevent parachute opening. This paper describes theoretical models as well as the results of small-scale wind tunnel experiments designed to confirm the validity of the models. Our ultimate goal is to extrapolate the models and experiments to full-size parachutes.

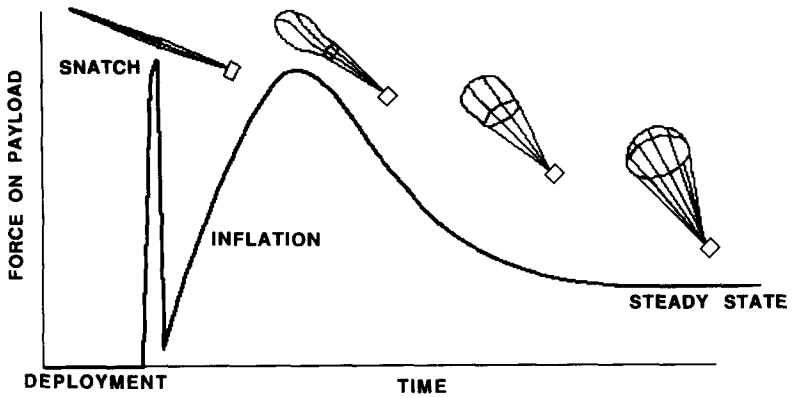

Fig. 1. Payload force versus time for a typical airborne parachute drop.

2. The three phases of a parachute drop

The various phases of a parachute drop generally consist of three principle stages: deployment, inflation, and steady-state [5]. The deployment phase begins with the ejection of the payload from the aircraft and ends when the suspension lines and folded canopy have been fully extracted from the deployment bag. The full extension of the parachute system is marked by the "snatch" force impulse, an event that occurs when the falling payload accelerates the parachute mass up to its own velocity. In most military airdrops, the deployment bag is attached to the aircraft by a static tether, hence the time lag between payload ejection and the snatch point is usually small. In free-fall personnel drops and sport parachute jumps, the time delay is usually longer. In either case, the parachute shape at the end of the deployment phase is essentially that of an elongated but uninflated tube.

During the subsequent filling, or inflation phase, the elongated parachute transforms from a closed tube to an open canopy, ultimately increasing the aerodynamic drag and decelerating the payload. Eventually, a steady state condition is reached where the aerodynamic drag balances gravity and the payload drifts to earth at a relatively constant velocity.

A typical plot of the force on the payload versus time during parachute opening is shown in Fig. 1. As this plot indicates, the force on the payload, with the exception of the snatch impulse, is small during the initial stages of inflation. As inflation continues, the opening force exerted by the continually filling canopy increases to a peak, then decreases over time. The small level of aerodynamic force associated with the early stages of post-deployment inflation is of particular interest from the point of view of electrostatics. At this stage of the opening process, the parachute shape is basically that of a thin, hollow, inwardly-collapsed tube that has the shape shown in the side view of Fig. 2 and the end view of Fig. 3. The parachute panels, called *gores*, remain folded and extend radially outward from the central axis. The folded gores initially

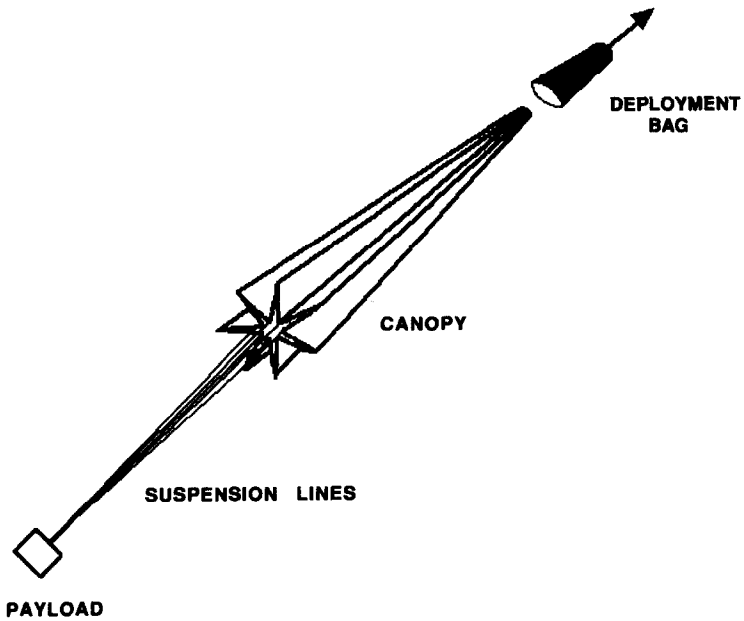

Fig. 2. Appearance of the parachute system just after the snatch impulse.

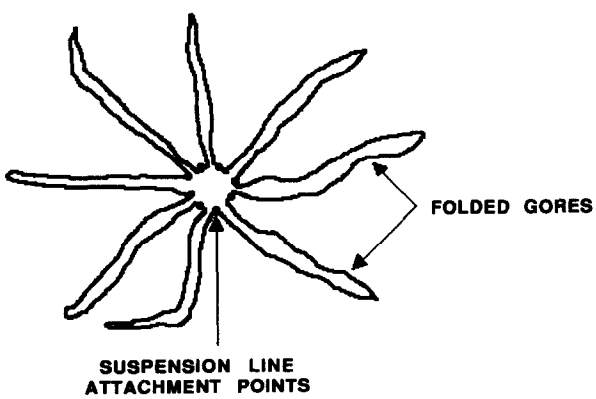

Fig. 3. Actual end view of parachute just after snatch. The dots represent the points of connection of the suspension lines.

remain closed and flutter about randomly, resulting in minimal aerodynamic drag force. At this stage of the opening process, any electrostatic forces that are present are likely to be large. The contacting layers of a folded gore, if oppositely charged, are the most susceptible to being held together by electrostatic attraction. In contrast, the

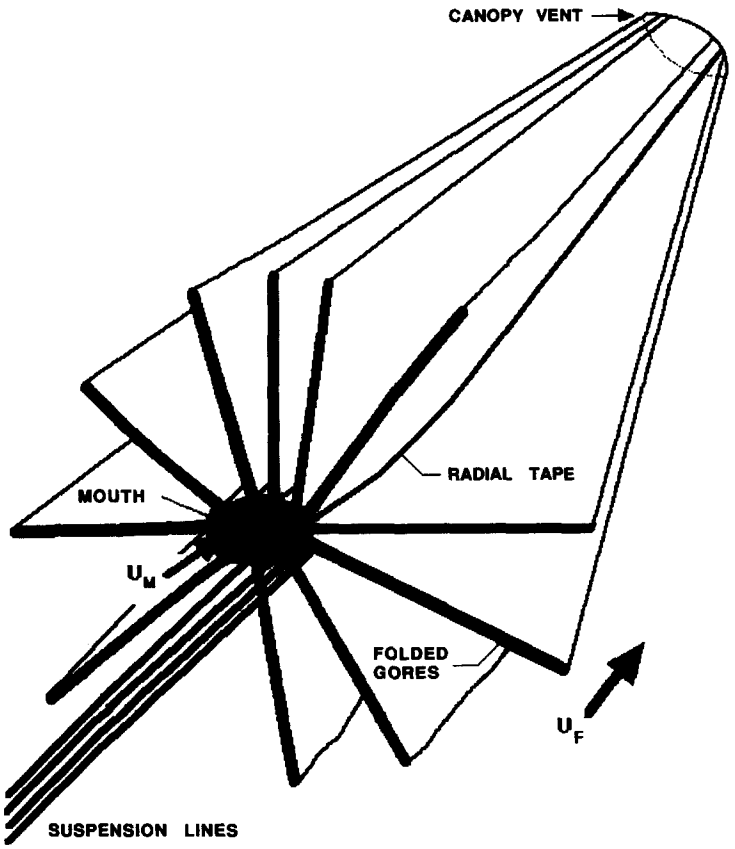

Fig. 4. Simplified model for the parachute just after snatch.

panels of a fully inflated canopy are widely separated and are unlikely to succumb to electrostatic forces. The early moments of the inflation phase just after snatch, therefore, are of most interest to the present study. However important a fully inflated canopy may be to human jumpers and strategic payloads, the later stages of inflation and the steady-state phase are the least interesting from the point of view of electrostatics.

3. Model for aerodynamic force just after snatch

The aerodynamic flow pattern around a parachute in the early stages of inflation is complex. Immediately after snatch, the flow may have laminar tendencies, but much of it is turbulent. Despite the probable complexity of the airflow, however, a great deal of insight can be gained by applying a simple laminar flow model to the simplified structure of Fig. 4. The parachute is represented as a two-dimensional structure with

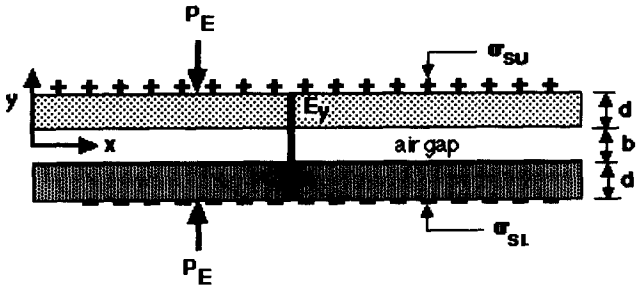

Fig. 5. Three-layer model for computing electrostatic forces between two pieces of charged cloth of thickness d separated by an air gap b.

no variation in the axial direction and is assumed to open radially outward from the center as the canopy inflates. High-speed photographs of real parachute drops [6] indicate this picture of the early stages of parachute opening to be a reasonable one. The central portion of the parachute, termed the mouth, is initially open by some amount regardless of airflow due to the physical presence of the suspension lines and attachment points. As the canopy inflates, the mouth widens and the folded gores peel apart. For a given mouth radius, the air velocity U_M into the mouth will be determined by the fill rate of the canopy. Since aerodynamic drag and deceleration during the deployment phase are minimal, the air velocity U_F outside the mouth just after snatch is assumed to be equal to the airspeed at the time of deployment.

The velocity difference across the walls of the mouth results in an outward aerodynamic pressure that can be expressed by the equation:

$$P_A = \tfrac{1}{2}\Gamma(U_F^2 - U_M^2), \tag{1}$$

where Γ is the density of air (1.2 kg/m^3 at 25 °C and 1 atm). The maximum P_A occurs when $U_M = 0$. The faster the fill rate of the canopy, the faster the mouth velocity U_M and the smaller the outward pressure P_A. At a typical airdrop velocity of $U_F = 65$ m/s (145 mph), the value of P_A with $U_M = 0$ becomes 2.5 kN/m^2. At $U_M = 50$ m/s, P_A drops to 1.03 kN/m^2; at $U_M = 60$ m/s, P_A drops to 0.4 kN/m^2. Even at this unlikely mouth velocity, the change in P_A from the $U_M = 0$ case is less than an order of magnitude. We may thus conclude that the assumption $U_M = 0$ is a reasonable one for estimating purposes in most parachute drops.

4. Model for electrostatic forces on a charged parachute

A zeroeth-order model suitable for providing an initial estimate of electrostatic forces is illustrated in Fig. 5. The opposing lower folds of the parachute gore, each of thickness d, carry uniform charge densities $\sigma_{sU} = \sigma_s$ and $\sigma_{sL} = -\sigma_s$, respectively, on their outer surfaces. The cloth faces are presumed to be separated by an air gap of thickness b. The downward-pointing electric field inside each nylon cloth layer,

obtained by simple application of boundary conditions, then becomes

$$E_n = -\sigma_s/\varepsilon_n, \tag{2}$$

where ε_n is the permittivity of the nylon cloth. Similarly, the field inside the air gap becomes $E_a = -\sigma_s/\varepsilon_0$. The attractive force between the two charged layers can be computed by first finding the energy per unit area stored in the system. The latter is given by

$$W_e = (2d)\frac{\varepsilon_n E_n^2}{2} + b\frac{\varepsilon_0 E_a^2}{2} = \frac{\sigma_s^2 d}{\varepsilon_n} + \frac{\sigma_s^2 b}{2\varepsilon_0}. \tag{3}$$

Taking the derivative of this energy with respect to the gap spacing b yields the attractive force per unit area, or electrical "pressure", acting on the cloth layers [7, 8]:

$$P_E = F_y = -\frac{dW_e}{db} = -\frac{\sigma_s^2}{2\varepsilon_0}. \tag{4}$$

For the purpose of comparing P_E with the previously calculated values of P_A, suppose that charge densities of $\sigma_{sU} = 10\ \mu C/m^2$ and $\sigma_{sL} = -10\ \mu C/m^2$ are assumed. These values are lower than the theoretical limit set by the breakdown strength of air, which is thought to apply to adjacent layers of the largely porous parachute cloth, and is lower than the Paschen limit for a gap on the order of 100 μm, the approximate thickness of standard parachute cloth. The assumed σ_s are also consistent with values obtained experimentally in the laboratory. Substituting these σ_s values into Eq. (4) results in $P_E = 4.9\ N/m^2$. This pressure is on the order of 100–1000 times smaller than the P_A estimates previously calculated for typical airdrop velocities.

5. Refined model for aerodynamic and electrostatic forces at the separation point

The preceding estimates of aerodynamic and electrostatic forces are useful for order-of-magnitude force comparisons, but a far more convincing picture can be found by focusing on the separation point at the inner edges of the folded gore where it intersects the circumference of the parachute mouth. This separation point marks the boundary between the mouth region, where the aerodynamic forces dominate, and the folded gore region, where electrostatic forces are maximum. As depicted in Fig. 6, the aerodynamic pressure acting to open the mouth causes a circumferential stress T_a to be exerted at the separation point. This stress, which acts to pull apart the edges of the folded gore, is analogous to "hoop stress" in a wooden barrel [10] and acts tangentially to the mouth circumference at the separation point. Note that T_a has dimensions of force per unit gore-edge length L, where L is perpendicular into the page in Fig. 6.

The magnitude of the "hoop stress" T_a of aerodynamic origin can be computed as follows: If the mouth has radius r, each increment of cloth of area $Lr\,d\theta$ around the mouth circumference will experience an increment of outward aerodynamic force

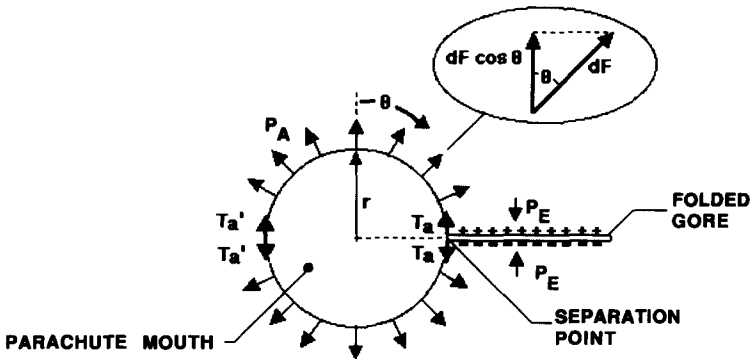

Fig. 6. Model for the parachute mouth, folded gore, and gore separation point. Only a single folded gore is shown. The outward aerodynamic pressure creates a hoop stress T_a that acts to peel the gore apart.

$dF = P_A L r\, d\theta$. The projection of this force component in the direction perpendicular to the gore plane can be expressed by

$$dF \cos\theta = P_A L r\, d\theta \cos\theta, \tag{5}$$

where θ is defined relative to the normal to the plane of the folded gore. The tension T_a per unit length at the separation point and its equal counterpart T_a' at the opposite side of the mouth, which represent the sum total of forces acting perpendicular to the gore plane, can thus be computed by integrating dF over half the mouth circumference:

$$L(T_a + T_a') = \int dF = P_A L r \int_{-\pi/2}^{\pi/2} \cos\theta\, d\theta = 2P_A L r. \tag{6}$$

By symmetry, $T_a' = T_a$, hence the total aerodynamic tension T_a per unit length acting on the gore edge becomes

$$T_a = P_A r \equiv \tfrac{1}{2}\Gamma(U_F^2 - U_M^2)r. \tag{7}$$

The folded gore will open when T_a exceeds the tension of electrostatic origin acting to hold it together. An estimate for the latter can be obtained from the "two slab" model of Fig. 7, in which any partially separated regions of the gore edges are represented by two oppositely charged, vertical slabs of cloth of height $\pm h$. The slabs are separated at their inner ends by a gap of distance $2g$. These slabs exert an attractive force on each other that directly opposes the hoop stress T_a. The electrostatic pressure contributed by the bulk of the layers remaining in contact acts normal to the cloth layers and does not counteract tension along the mouth circumference. Similarly, the repulsion force exerted by a given slab on itself has no net component and may be ignored.

The attractive force between slabs can be computed by considering the coordinate system of Fig. 7. An incremental charge element $\sigma_{sU} L\, dy$ on the upper slab will

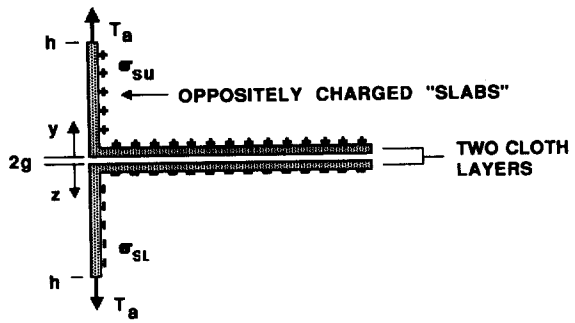

Fig. 7. Two-slab model for estimating electrostatic forces at the gore separation point.

experience a force equal to

$$dF_y = \int_{z=g}^{z=h} \frac{(\sigma_{sU} L\, dy)(\sigma_{sL}\, dz)}{2\pi\varepsilon_0 (y+z)}. \tag{8}$$

Here σ_{sU} and σ_{sL} are again the charge densities on the upper and lower slabs, respectively. The charge densities σ_{sU} and σ_{sL} could vary with position, but they are assumed to be uniform without loss of generality. The integral (8) is equivalent to a summation of the forces felt by a line charge of magnitude $\sigma_{sU}\, dy$ and length L due to the field of a series of line charges of magnitude $\sigma_{sL}\, dz$ that make up the lower slab. Note that dF_y will be negative (attractive) when σ_{sU} is positive and σ_{sL} negative.

Integration of Eq. (8) over z using an appropriate change of variables results in

$$dF_y = \frac{\sigma_{sU}\sigma_{sL}}{2\pi\varepsilon_0} L\, dy \ln\frac{y+h}{y+g}. \tag{9}$$

The total force on the upper slab can then be found by integrating dF_y from $y = g$ to $y = h$:

$$F_y = \int_{y=g}^{y=h} \frac{\sigma_{sU}\sigma_{sL}}{2\pi\varepsilon_0} L \ln\frac{y+h}{y+g}\, dy. \tag{10}$$

With several changes of variable and the substitution $\int \ln x\, dx = x(\ln x - 1)$, Eq. (10) can, after some algebra, be reduced to

$$F_y = \frac{\sigma_{sU}\sigma_{sL}}{2\pi\varepsilon_0} L\, 2h\left[\ln\frac{2h}{h+g} + 2d\ln\frac{2g}{h+g}\right]. \tag{11}$$

In the limit $g \ll h$ (gap separation negligible compared to slab height), the second term approaches zero, resulting in

$$F_y \approx \frac{\sigma_{sU}\sigma_{sL}}{2\pi\varepsilon_0} L(2h)\ln 2. \tag{12}$$

This equation is linear in slab height h. Dividing it by the gore length L results in an expression for the electrostatic tension per unit length due to Coulomb attraction:

$$T_e = \ln 2 \frac{\sigma_{sU}\sigma_{sL}}{\pi\varepsilon_0} h. \tag{13}$$

Note that the above model predicts an electrostatic force exerted only by the peeled, exposed portions of the parachute gore. In contrast to the crude electrostatic force model of Section 4, the force contribution due to the layers of cloth remaining in contact is essentially zero. To the extent that separation at the gore edges can be modeled by two perpendicular, oppositely charged slabs, the threshold conditions for parachute opening can be found by finding the conditions under which $T_e + T_a = 0$, i.e., from Eqs. (7) and (13):

$$\sigma_{sU}\sigma_{sL} h \frac{\ln 2}{\pi\varepsilon_0} = \tfrac{1}{2}\Gamma(U_F^2 - U_M^2)r = P_A r. \tag{14}$$

Solving Eq. (14) for P_A subject to the condition $\sigma_{sU} = -\sigma_{sL} = \sigma_s$ yields the minimum Bernoulli pressure P_A needed to open the parachute for a given surface charge density $\pm\sigma_s$:

$$P_A = \sigma_s^2 \frac{\ln 2}{\pi\varepsilon_0} \frac{h}{r}. \tag{15}$$

For an assumed charge density of $\sigma_s = 10\ \mu C/m^2$, typical mouth radius of $r = 25$ cm, and slab height of $h = 10$ cm, the critical opening pressure becomes $P_A \approx 1\ N/m^2$. This value for P_A is again a factor of about 10^3 below the values of P_A calculated at a typical airdrop velocity.

The relationship between T_a and T_e can also be expressed in terms of the minimum airspeed velocity $U_F = U_{min}$ required to open a charged parachute. For zero mouth velocity ($U_M = 0$) and fixed charge densities $\pm\sigma_s$, Eq. (14) becomes

$$\frac{\Gamma U_{min}^2}{2} = \sigma_s^2 \frac{\ln 2}{\pi\varepsilon_0} \frac{h}{r} \tag{16}$$

or

$$U_{min} = \sigma_s \left[(2 \ln 2) \frac{h}{\Gamma \pi \varepsilon_0 r} \right]^{1/2}. \tag{17}$$

Substitution of the representative values $\sigma_s = 10\ \mu C/m^2$, $r = 25$ cm, $h = 10$ cm, and $\Gamma = 1.2\ kg/m^3$ results in $U_F \approx 1.3$ m/s $\equiv 2.9$ mph. This velocity is well below those encountered during typical airdrops.

The relationship between T_a and T_e can be further manipulated into a form that can be used to determine the minimum charge needed to prevent gore opening at a realistic deployment airspeed U_F. For the typical value $U_F = 65$ m/s (about

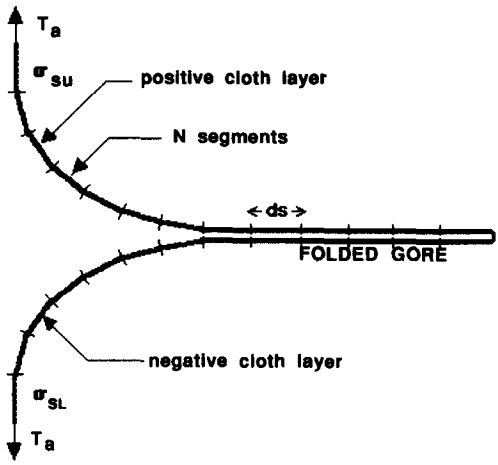

Fig. 8. Discretized representation of a peeling gore. Each layer of cloth is represented by N strip segments of width ds and length L into the page.

145 mph) with $U_M = 0$ and $\sigma_{sU} = -\sigma_{sL} = \sigma_s$, the minimum charge needed to prevent opening becomes

$$\sigma_s = \left| \frac{\Gamma U_F^2 \pi \varepsilon_0 r}{2h \ln 2} \right|^{1/2} = 500\ \mu C/m^2. \tag{18}$$

This value of charge lies well above the fundamental limit of 27 $\mu C/m^2$ set by the breakdown strength of air – a limit thought to apply to the semi-porous parachute cloth – but is not an unrealistic value for a solid nylon dielectric. The issues of maximum possible charge density, the mechanisms by which such charge might be deposited, and the conditions under which it might remain on the parachute fabric are questions that are the subject of studies now in progress.

Note that at large ratios of h/r, the "slabs" used in the above model form a significant portion of the mouth circumference and will no longer be perpendicular to the gore planes. Under these conditions, the simple two-slab model breaks down. For small slab heights, however, representative of a parachute at the early stages of opening (folded gores just beginning to be peeled apart), the result provides a useful measure of the threshold conditions for gore opening.

6. Numerical simulation of the gore peeling process

A more detailed numerical analysis of the gore peeling process has underscored the validity of the simple two-slab model. Two layers of oppositely charged cloth, initially in planar contact, form the faces of a single folded gore. As illustrated in Fig. 8, each layer is modeled as a series of N discrete strips of width ds and length L. Each strip

carries a constant charge $\sigma_s\,ds$ per unit length, where σ_s is the charge per unit area on the cloth at the location of the strip. For simplicity, symmetry about the plane of the folded gore with $\sigma_{sL} = -\sigma_{sU}$ is assumed, so that the negatively charged cloth becomes the mirror image of the positively charged cloth.

The numerical calculations were performed using a custom program written in the MATLAB programming language. The details of the computational method are described elsewhere [9]. The simulation begins with tensions $\pm T_a$ per unit length applied at the gore edges at an angle of 90° relative to the gore plane, as illustrated in Fig. 8. As the simulation evolves over time, the Coulomb force acting on each strip is computed as the sum of force contributions from all other strips in the problem. Beginning with the edge strips to which $\pm T_a$ are applied, the tension component transmitted from each strip to its next-nearest neighbor is determined by the relative angles between strips. Gravity, thought to have a minor influence on the opening process, is ignored. The Coulomb force is then added to the mechanical tension force. The net component of force acting perpendicular to each strip, including the Coulomb force, is computed, and the position of each strip relative to the gore plane adjusted by an arbitrarily small but proportional increment. The position adjustments are made subject to the constraint that the total contour length of the cloth remain constant. The iteration is repeated over all strips in the contour until either force equilibrium is reached along the entire contour (electrostatic forces hold back tension forces; gore fails to fully open) or until the gore edges become fully extended in the directions of $\pm T_a$ (electrostatic forces overcome by tension; gore opens). This numerical method closely models the actual physical process that occurs when tension forces act to separate two pieces of charged cloth. The problem is similar to the classic catenary problem of the suspension bridge [10], but in this case electrostatic forces replace the customary gravity force. In both cases, the stiffness modulus of the material is ignored, such that the resulting contour is caused only by the external forces acting on the material.

Results of the simulation involving applied tensions in the range 0.1–5 N/m and a charge density of $\sigma_s = 10^{-6}$ C/m^2 are illustrated in Fig. 9. The heights of the peeled cloth at which the electrostatic force just balances the applied tension T_a are summarized in Table 1. Also included in the table are the peeled heights at force balance predicted by the simpler two-slab model of the previous section for these same values of T_a and σ_s. The results indicate that the simpler two-slab model provides a reasonable estimate of the actual electrostatic forces associated with a peeling gore, and hence may be used in rough estimates of the minimum deployment airspeed required to open a parachute.

The plots of Fig. 9 all appear to predict right-angle contours at the separation point. A blown-up detail of the separation point for the representative case $T_a = 0.1$ N/m and $\sigma_s = 10^{-6}$ C/m^2, shown in Fig. 10, indicates that the profile is close to a perfect right angle, but in fact follows a tall and narrow catenary-like profile. The simulated contours are not unlike those physically observed in peeling experiments performed on real samples of cloth. They indicate that, contrary to our original expectations, the long-range effects of the electrostatic charge have little influence on the contour shape at the separation point but only contribute to the overall electrostatic tension.

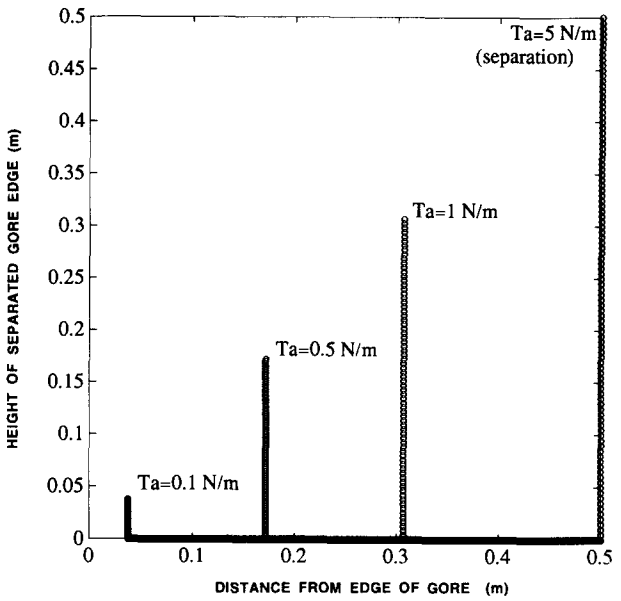

Fig. 9. Results of numerical simulation based on the segmented model of Fig. 8. Each plot represents the height of the peeled gore at which the tension T_a of aerodynamic origin is balanced by the force of electrostatic origin.

Table 1
Height of peeled gore segments at force equilibrium vs. applied tension for $\sigma_s = 10^{-6}\,C/m^2$

T_0 (N/m)	Height predicted by two-slab model (m)	Height predicted by contour simulation (m)
0.1	0.04	0.039
0.5	0.2	0.18
1.0	0.4	0.32
5.0	Separation	Separation

7. Small-scale wind tunnel tests

Full-size airdrop tests on charged parachutes under actual airdrop conditions are difficult to perform. We chose instead to test our theory via a series of wind tunnel tests at 5–20 mph (2.2–8.9 m/s) using a small-scale 36 in. (0.9 m) diameter, six-gore parachute made from 0.003 in. (80 μm) thick, low porosity nylon (US military specification MIL-C-44378-T/I). No attempt was made to apply general aerodynamic scaling laws to the parachute. Rather, our approach was to calculate the aerodynamic and electrostatic forces for the model parachute and to then predict the parachute's minimum opening airspeed. The agreement between our theory and data serves as

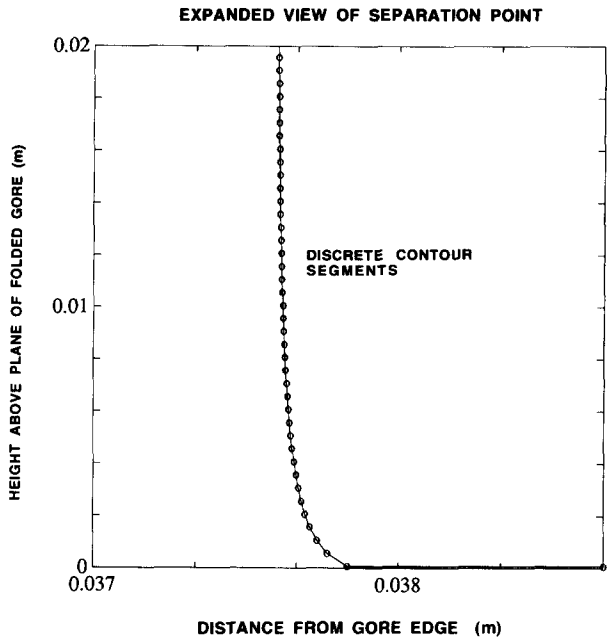

Fig. 10. Expanded view of the $T_a = 0.1$ N/m plot of Fig. 9 shows that the calculated contour has catenary-like profile.

a confirmation of the theoretical model which we hope to extrapolate to full-size charged parachute tests in the future.

Prior to each test, the parachute was neutralized by scanning it with a charge-balanced forced air volume ionizer. The parachute was then installed in the test fixture of Fig. 11. The six gore panels were folded in half, three on each side of the test fixture, with the suspension lines concentrated in the center. A 0.02 in. (500 μm) thick paper-board–aluminum foil–paperboard sandwich was inserted inside each folded gore to function as an isolating electrical spacer between upper and lower cloth faces. Just prior to release, the opposing sides of all folded gores were simultaneously charged to opposite polarities using 8 μm-wire stainless steel fiber brushes in direct contact with the fabric. The brush potentials were alternately set at 2–4 kV and ground, as illustrated in Fig. 12. (The brushes are also labeled in the photograph of Fig. 11.) The energized brushes and their grounded counterparts were swept once aross the surfaces of the folded gores for a duration of about 20 s. The paperboard insulators permitted the layers of each folded gore to sustain the potential difference between the contacting brushes. This charging method was observed in separate experiments to deposit nearly uniform and opposite charge densities on opposing cloth layers.

During the charging operation, the foil layer inside each paperboard sandwich was allowed to float electrically to a potential midway between the high-voltage brush potential and the grounded brush potential. After charging, the foil was grounded

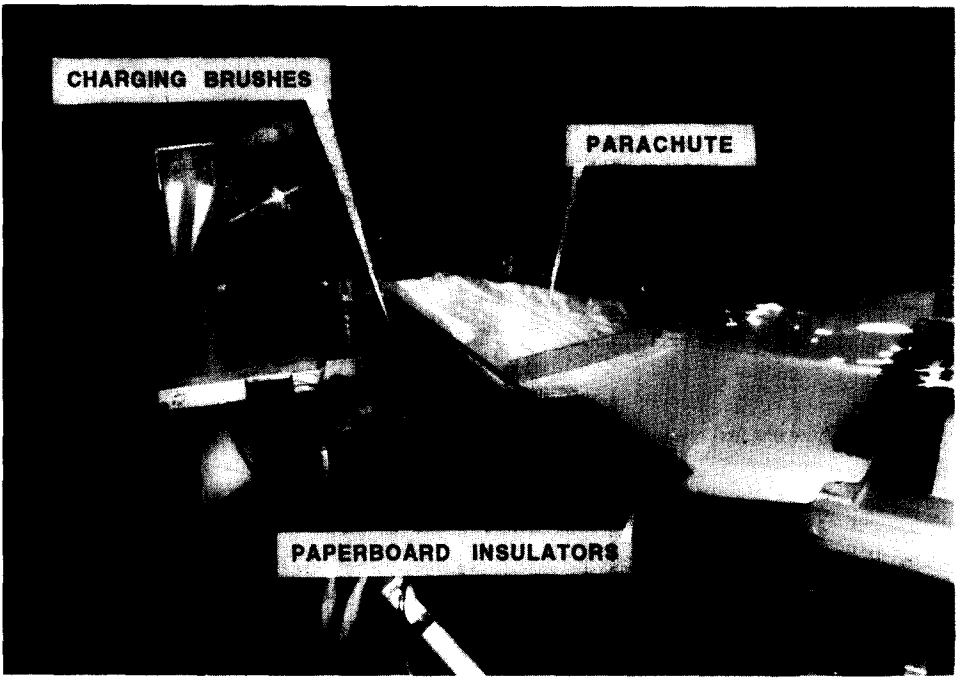

Fig. 11. View of test fixture for small-scale parachute tests.

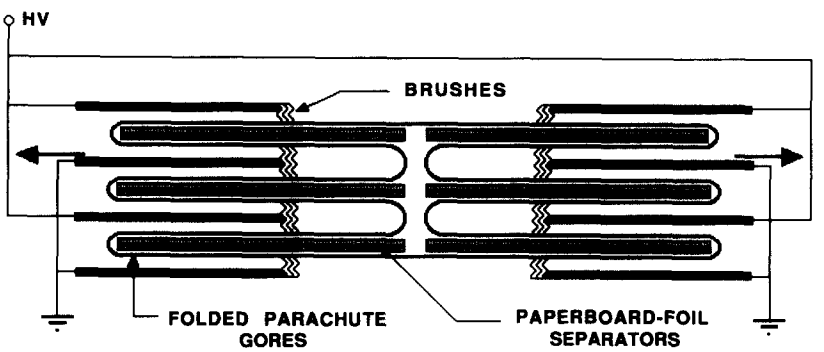

Fig. 12. Charging brush arrangement.

externally to provide a reference plane against which the charge magnitude on the cloth could be measured. Such measurements were performed just prior to release using a Monroe-type noncontacting voltmeter. The charge density was determined from the measured surface potential using the relation [11] $\sigma_s = V[d_p/\varepsilon_p + d_n/\varepsilon_n]^{-1}$,

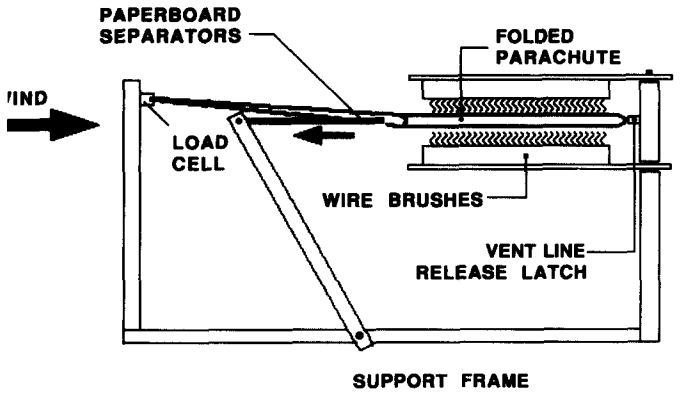

Fig. 13. Parachute test fixture showing removal of paperboard separators. Overall length is approximately 2 m.

where V is the measured surface potential, ε_p and d_p the permittivity and thickness of the paperboard, and ε_n and d_n the permittivity and thickness of the nylon cloth. The permittivity of paperboard was measured in a separate experiment using a 10 cm diameter test cell at 10 Hz and found to be about $2.3\varepsilon_0$ – a value we assumed to apply to dc conditions. The permittivity of the nylon cloth was similarly measured and found to be equal to about $1.3\varepsilon_0$. The charge deposited by this brush technique spanned the range from 5 to 20 $\mu C/m^2$ from test to test, with an average of about 10 $\mu C/m^2$. Since it was not possible to directly measure the charge density on the middle and lower gores in Fig. 12 without disassembling the parachute, we assumed the charge density measured on the upper layer of the top gore to be representative of the charge on all the gores in the folded parachute. This assumption was qualitatively confirmed in several post-inflation tests by measuring equal relative electric field magnitudes around the gores of the parachute after inflation with a noncontacting field meter probe held at a fixed distance from the cloth. The question of whether our deposited charge densities represent the maximum physically possible remains unresolved and is the focus of work now in progress.

Prior to release in the air stream, the flat folded parachute was held shut by two skirt clamps. After longitudinal removal of the paperboard separators, as depicted in Fig. 13, the skirt clamps were quickly retracted and the vent line released, thus freeing the parachute to interact with the ambient air stream under infinite-mass (constant air velocity) conditions, as in Fig. 14. In order to determine the time between release (force minimum) and full opening (steady-state force) the net drag on the parachute was monitored using a load cell attached between the ends of the suspension lines and the stationary test fixture.

The results of these experiments, which involved over forty trials, are summarized in Fig. 15. At 5 mph (2.2 m/s), the charged parachute failed to open every time. At 10 mph (4.5 m/s), the opening time of the charged parachute was always longer than the uncharged opening time, and one failure to open was observed. At 15 mph

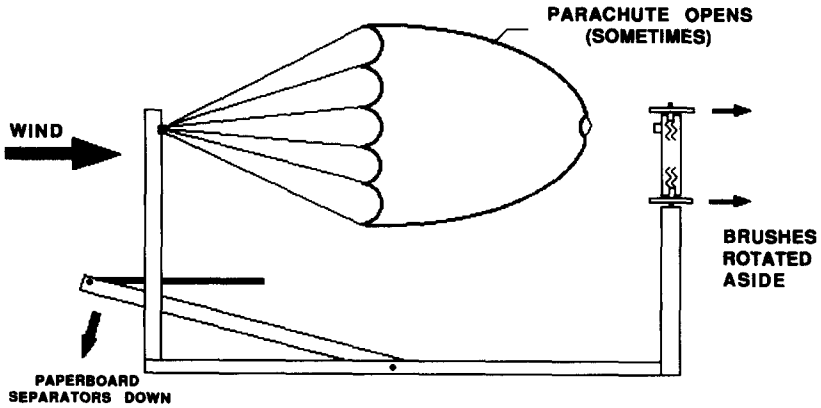

Fig. 14. Parachute in test fixture after release.

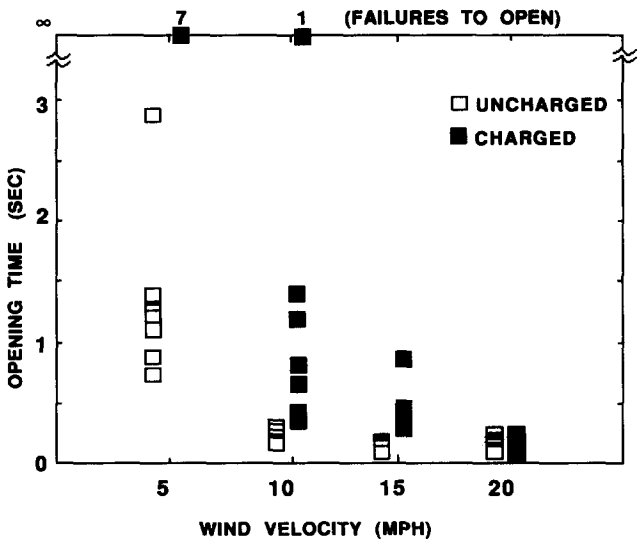

Fig. 15. Summary of test results. Opening times of charged and uncharged small-scale parachute at various wind velocities.

(6.7 m/s), no total failures to open were observed, but most of the charged tests exhibited some delay in opening. At 20 mph (8.9 m/s), charged and uncharged opening times followed essentially the same statistical distribution. From these tests, we conclude that the minimum air velocity for the opening of our charged model parachute lies somewhere between 5 and 10 mph for our set of test conditions.

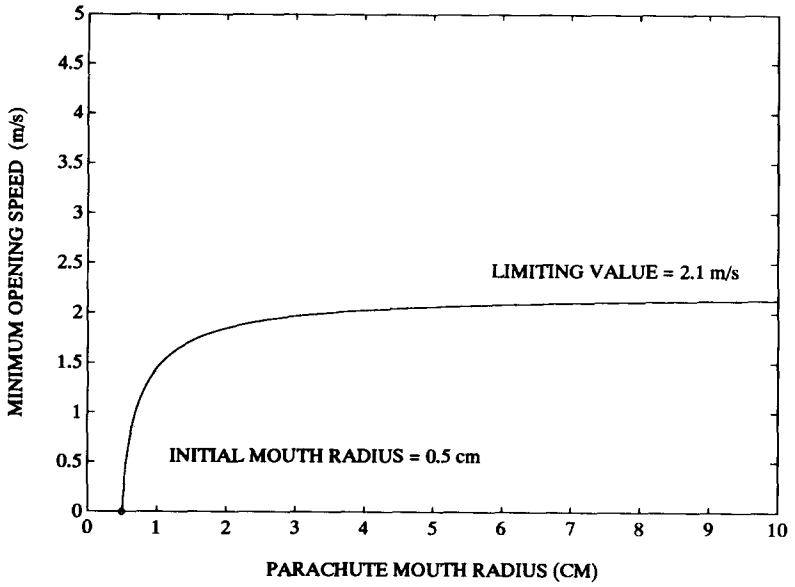

Fig. 16. Calculated value of air velocity at which aerodynamic and electrostatic forces in the small-scale parachute balance versus parachute mouth radius. Assumed parameters: $\sigma_s = 10\ \mu C/m^2$, $U_M = 0$.

8. Comparison of theory and data

The theoretical model summarized by Eq. (14) was tested against the experimental results by assuming the parachute mouth immediately after release to be fully closed. Under the assumption $U_M = 0$, Eq. (14) was used to compute the minimum air speed U_{min} needed to open the parachute at successively larger mouth radii. At a given mouth radius, the lengths of the exposed "charge slabs" were equated with the net increase in mouth circumference. A plot of the calculated U_{min} versus increasing mouth radius for an assumed surface charge density $\sigma_s = 10\ \mu C/m^2$ is shown in Fig. 16. As is evident in the figure, the curve approaches the value $U_{min} \approx 2.1$ m/s (4.8 mph) as the parachute opens and the mouth radius increases. For airspeeds below this value, electrostatic forces will balance aerodynamic forces at some value of radius, resulting in a parachute that fails to completely open. Our experimentally determined minimum opening speed, which lies between 5 and 10 mph, is within the range of this theoretically determined value. Given the simple nature of the theoretical model, our assumption that $U_M = 0$, and the fact that the small parachute quickly departs from a two-dimensional structure as the parachute opens, the rough agreement between the model and the experimental data shows that the former can provide a reasonable estimate of the minimum airspeed required to fully open a charged parachute. Note that the above models are based entirely on static force equilibrium. No attempt has been made to model the dynamics of the opening process, hence no statement can be made regarding the ability of electrostatic charge to *slow down* parachute opening even when the airspeed is sufficiently large to open the parachute.

9. Conclusions

A simple theory for parachute opening based on Bernoulli's equation has been combined with a two-slab model for the electrostatic force exerted by separated regions of charged parachute fabric. The validity of this two-slab model has also been confirmed by detailed numerical simulations. The combined aerodynamic and electrostatic force models have been used to predict the minimum deployment airspeed needed to open a parachute with oppositely charged gore faces. The predictions of the combined models have been verified experimentally in wind tunnel tests. Our experiments indicate that electrostatic forces on a small-scale parachute charged to $\pm 15\,\mu C/m^2$ can prevent parachute opening at air speeds below about 10 mph (4.5 m/s).

10. Nomenclature

ε_n	dielectric permittivity of nylon cloth
ε_p	dielectric permittivity of paperboard
Γ	density of air
σ_s	surface charge
b	thickness of air space between parallel cloth layers
d, d_n	thickness of cloth layer
d_p	thickness of paperboard
dq	increment of charge
F	force
g	gap separation at inner ends of two vertical slabs of cloth
h	height of charge slabs used to model peeling gore
L	longitudinal length of parachute gore
P_A	aerodynamic pressure
P_E	electrostatic pressure
r	radius of parachute mouth opening
T_a	tension per unit length of aerodynamic origin
T_e	tension per unit length of electrostatic origin
U_F	ambient air velocity around parachute
U_M	air velocity into mouth of a parachute
U_{min}	minimum air velocity needed to overcome electrostatic forces
W_e	stored energy per unit area

Acknowledgements

The authors would like to acknowledge the assistance of James Fairneny, Gary Vincens, Christina Udelson, and Daniel Litvack, who assisted with the experiments,

and the helpful insights contributed by Thomas Godfrey, Louis Piscitelle, and Calvin Lee.

References

[1] W.D. Brown, Parachutes, Pitman, London, 1951.
[2] J.W. Sweeney, Evaluation of Antistatic Agents on Nylon Parachute Cloth, Lowell Technological Institute Research Foundation, Sept. 1955, Project No. 7320, Wright Air Development Center WADC TR 54-513 (NTIS AD-090 581).
[3] Airdrop Review and Malfunction/Safety Analysis, Vols. I and II (1991), Vols. II and III (1987); Vol. III (1985); Commander, US Army Quartermaster Center and School, Fort Lee, VA 23801-5038; ATTN: ATSM-ABN-FS.
[4] C.T. Davey, J.F. Heffron and J.L. Christopher, The Effects of Static Electrification on Airdrop Systems, US Army Natick Research and Development Center, Sept. 1983, NATICK/TR-85/015L (NTIS AD B-090 1831).
[5] J.D. Cockrell, The Aerodynamics of Parachutes, Advisory Group for Aerospace Research and Development (NATO-AGARD), AGARD-AG-295, 1987, p. 44.
[6] M. Horenstein and N. Roberts, Comparison of aerodynamic and electrostatic forces during parachute opening, J. Aircraft, 24(12) (1994).
[7] H. Woodson and J.R. Melcher, Electromechanical Dynamics, Wiley, New York, 1968.
[8] M. Zahn, Electromagnetic Field Theory: A Problem Solving Approach, Wiley, New York, 1979, pp. 221–223.
[9] M. Horenstein and N. Roberts, Peeling force for an electrostatically charged sheet on a grounded surface, 1993 IEEE Industry Applications Society Annual Meeting, October 4–7, Toronto.
[10] F. Seely and N.E. Ensign, Analytical Mechanics for Engineers, Wiley, New York, 1941.
[11] R.M. Schaffert, Electrophotography, Wiley, New York, 1975.